Lightweight multi-degree-of-freedom displacement-sensing link shells for safe and intuitive physical human-robot interaction

Gabriel Boucher[a], Thierry Laliberté[a] and Clément Gosselin[a]

***Abstract*— This paper introduces novel displacement-sensing link shells for the physical interaction between a human user and a serial robotic arm. The approach is inspired from the concept of macro-mini robot architecture. The framework is developed for a general multi-degree-of-freedom serial robot and a corresponding impedance control scheme is proposed. The concept is demonstrated using a five-degree-of-freedom robotic arm equipped with a six-degree-of-freedom low-impedance sensing shell that is used to control the robot. Experimental results are provided.**

I. INTRODUCTION

Physical human-robot interaction can be achieved using a variety of approaches. Impedance control is a popular technique to enable the collaboration between humans and robots [1]. The user applies a force on the robot and moves it: this movement can be measured and used in a control law to make the robot follow a given behaviour. The drawback of this approach is that the user feels the impedance of the robot, which therefore needs to be low. Also, the robot must be backdrivable, which is often not the case since robots typically use harmonic drive transmissions.

An alternative approach to enable human-robot collaboration is admittance control, which consists in using force/torque sensors to detect collisions or to gather feedback on the physical interaction between the robot and a human user [2][3][4]. In fact, this type of control can be thought of as a form of impedance control —with very high impedance— because the force measured is inferred from a displacement on a much smaller scale (usually the deformation of a strain gauge). In this case, the displacement required is so small that the robot virtually does not move. A drawback of this approach is that the user feels the delay of the control loop and that force or torque sensors are noisy and often suffer from drift.

Yet another approach that is used to enable human-robot collaboration is the use of a macro-mini architecture [5][6]. In some implementations, the macro manipulator is an active manipulator while the mini manipulator is passive and is used to control the robot. In some cases, the mini manipulator also supports the payload [7][8][9]. The user moves the passive mini-manipulator which is a low-impedance mechanism, and the displacement between the macro and mini manipulators is used to control the actuated macro manipulator.

The authors would like to acknowledge the financial support of the Natural Sciences and Engineering Research Council of Canada (NSERC) and of the Canada Research Chair program.

[a]Département de génie mécanique, Université Laval, 1065 Avenue de la Médecine, Québec, Qc, G1V 0A6, Canada, gabriel.boucher.3@ulaval.ca, thierry@gmc.ulaval.ca, gosselin@gmc.ulaval.ca

The drawback of the kind of macro-mini manipulators presented in [7][9] is that the low-impedance passive mechanism must support the weight of the payload and must be structurally robust. Furthermore, when interacting with the low-impedance mechanism, the user feels the inertia of the payload which has the effect of increasing the impedance of the mechanism if the payload is large.

A similar concept is presented here, where a low-impedance lightweight sensing device is mounted on the links of a serial robot. The user then physically interacts with the robot through a very light link shell instead of being in direct contact with the structural links of the robot. Compared to existing collaborative robots in which the torques at the joints are measured (including the gravitational and inertial loads at the robot joints), the proposed approach has the advantage of directly measuring the interaction between the robot and user without 'drowning' the measurements in large gravitational or inertial loads. Moreover, instead of measuring the micro displacement of strain gauges (high impedance interface), the proposed approach relies on the measurement of displacements of the order of 1 cm, which yields a very low impedance and provides a very intuitive and immediate reaction. Also, compared to the macro-mini architecture, the proposed approach has the advantage of being independent from the payload and relying on small low-impedance components that do not play a structural role in the robot. The readings of the low-impedance sensing device are therefore limited to the user input and do not require any compensation or filtering. The new concept is briefly presented in this paper. Also, a six-degree-of-freedom (6-dof) sensing device and a 5-dof serial robot are developed and built in order to illustrate the application of the concept. Experimental results are also provided to demonstrate the effectiveness of the low-impedance interaction.

II. SENSING APPROACH

A. Sensing principle

In conventional collaborative robots, the force applied by the user is inferred by measuring the joint torques, as illustrated in Fig. 1. In such an approach, the user interacts directly with a relatively high impedance system, which limits the reactiveness. As mentioned above, gravity and inertial loads due to the robot links and payload are included in the torque measured at the joints. These loads can be significantly larger than the loads produced by the user interaction, if a comfortable interaction is desired.

The concept proposed here, illustrated in Fig. 2, consists in decoupling the user interaction loads from the gravi-

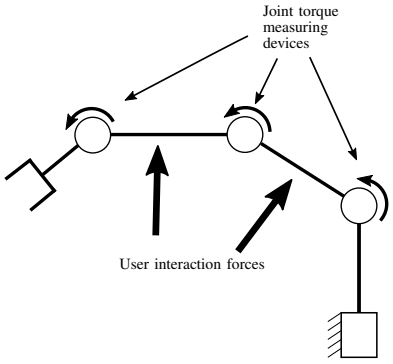

Fig. 1. Conventional collaborative robot with torque sensors at the joints.

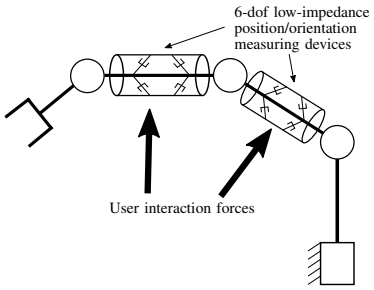

Fig. 2. Proposed collaborative robot with position/orientation sensors in parallel mounted on the links.

tational and inertial loads of the robot and payload via low-impedance multi-dof sensing shells mounted on the links of the robot. The shells are connected to the robot via passive parallel mechanisms that are used to measure the displacement (position and orientation) of the shells with respect to the links. The passive parallel mechanisms are equipped with elastic return devices that return to the reference configurations when no external load is applied to the shells. Using this arrangement, the user loads are decoupled from the gravitational and inertial loads due to the robot and the payload. By using the low-impedance sensing devices to measure the position and orientation of the shells with respect to the robot links, the interaction with the user has a low impedance which allows for a high responsiveness. The motion of the shells is mapped into the motion of the robot using a procedure that is explained in the following sections.

B. Reaction capabilities

The relationship between the Cartesian velocity vector $\mathbf{t}$ and the actuator velocity vector $\dot{\boldsymbol{\theta}}$ in a serial robot is given by

$$\boldsymbol{t} = \boldsymbol{J}\dot{\boldsymbol{\theta}} \tag{1}$$

where $\boldsymbol{J}$ is the Jacobian matrix of the robot and where the joint velocity vector is constrained as

$$\dot{\boldsymbol{\theta}} \preceq \dot{\boldsymbol{\theta}}_{\max} \tag{2}$$

where $\preceq$ stands for the componentwise inequality. For a given configuration of the robot, (1) and (2) define a polytope that provides the Cartesian velocity limits [10]. This polytope can be used to determine the capabilities of the robot in a given Cartesian direction, which can then be used to determine the bandwidth provided by the low-impedance sensor. This can be used when planning a task in order to determine what configuration would be the most suitable for the robot, similarly to how one would use the sensitivity index to plan a precise task. A similar analysis can be done for the accelerations of the robot.

III. Control scheme

A. Control loop

The basic inner control loop is based on a simple position controller. The position error can be expressed as

$$\boldsymbol{e} = \boldsymbol{\theta}_{ref} - \boldsymbol{\theta} \tag{3}$$

where $\boldsymbol{\theta}_{ref}$ is the desired joint position vector and $\boldsymbol{\theta}$ is the actual joint coordinate vector. This error is used in a controller to obtain a torque to control the motors, namely

$$\boldsymbol{\tau} = \boldsymbol{K}_p\boldsymbol{e} + \boldsymbol{K}_d\dot{\boldsymbol{e}} + \boldsymbol{g}(\boldsymbol{\theta}) \tag{4}$$

where $\dot{\boldsymbol{e}}$ is the time derivative of the position error and $\boldsymbol{g}(\boldsymbol{\theta})$ is the gravity compensation term. $\boldsymbol{K}_p$ and $\boldsymbol{K}_d$ are the proportional and derivative coefficient matrices respectively. If the robot is used to follow a prescribed trajectory, then $\boldsymbol{\theta}_{ref}$ is prescribed by a trajectory planning algorithm. However, if the robot is controlled using the passive interaction mechanism, determining the appropriate value of $\boldsymbol{\theta}_{ref}$ requires some preprocessing. In this case, the displacement of the passive mechanism can be used to obtain a reference velocity as

$$\boldsymbol{v}_{ref} = \boldsymbol{K}_{ps}\Delta\boldsymbol{x} + \boldsymbol{K}_{ds}\Delta\dot{\boldsymbol{x}} \tag{5}$$

where $\boldsymbol{K}_{ps}$ and $\boldsymbol{K}_{ds}$ are respectively the proportional and derivative coefficient matrices and $\Delta\boldsymbol{x}$ and $\Delta\dot{\boldsymbol{x}}$ are the displacement of the low-impedance sensing device and its time derivative.

The Cartesian reference velocity obtained from (5), $\boldsymbol{v}_{ref}$, is then mapped onto the joint space of the robot using the Jacobian matrix $\mathbf{J}$ of the robot, namely

$$\dot{\boldsymbol{\theta}}_{ref} = \boldsymbol{J}^{-1}\boldsymbol{v}_{ref}. \tag{6}$$

The prescribed position in the joint space $\boldsymbol{\theta}_{ref}$ is then obtained by integrating the velocity over one time step and the resulting value of $\boldsymbol{\theta}_{ref}$ is used in the motor controllers to move the robot. In summary, the measured displacement of the shell mounted on a link is used to calculate a velocity command which is then integrated and used as a control input for the low-level position control of each of the motors. The global control scheme is illustrated in Fig. 3.

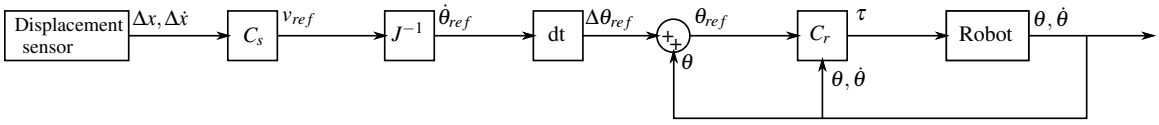

Fig. 3. Control loop of the system. C_s is the controller used on the sensor displacement and C_r is the low-level position controller.

B. Mapping of the desired motion onto the joint space and use of the damped pseudo-inverse

The above derivation assumes that the robot is not in a singular configuration. It also assumes that the number of degrees of freedom of a given link, on which the low-impedance shell is mounted, matches that of the connection (displacement sensor) mounted between the shell and the link. However, in the proposed implementation, 6-dof passive mechanisms can be used to connect the shells to the links, even for links that have fewer than 6 degrees of freedom. Therefore, in such cases, the Jacobian matrix associated with the link on which the sensor is mounted has fewer columns than rows. For instance, consider the third moving link of a serial robot. The Jacobian matrix associated with this link has 6 rows and 3 columns. If a 6-dof displacement sensor is mounted on this link, the displacements measured by the sensor are generally not compatible with the available three dofs and have to be mapped onto the motion that can be produced by the first three joints of the robot to produce the required motion as closely as possible. Equation (6) is then replaced with

$$\dot{\boldsymbol{\theta}} = (\boldsymbol{J}^T\boldsymbol{J})^{-1}\boldsymbol{J}^T\boldsymbol{t} \tag{7}$$

which is the least square solution to (1). The resulting joint motion produces the Cartesian motion that is as close as possible to the requested motion, in the sense of the least squares, which produces an intuitive behaviour. Additionally, in singular configurations, matrix $\boldsymbol{J}$ becomes rank deficient. In this case, even the formulation of (7) fails. In order to alleviate this problem, the concept of damped pseudo-inverse [11] is used. Indeed, near singular configurations the joint velocities required in order to produce a certain Cartesian velocity can become very high which is not desired, especially when dealing with collaborative robots. The solution based on the damped pseudo-inverse can be expressed as

$$\dot{\boldsymbol{\theta}} = (\boldsymbol{J}^T\boldsymbol{J} + \alpha\boldsymbol{I})^{-1}\boldsymbol{J}^T\boldsymbol{t} \tag{8}$$

where α is the damping coefficient and $\boldsymbol{I}$ is the identity matrix. The formulation of (8) is very similar to that of (7). In fact, it is identical if α is equal to zero, but the addition of the damping term $\alpha\boldsymbol{I}$ prevents the matrix from becoming singular which stabilises the solution. Parameter α is generally tuned experimentally on the real robot and it can also be modified online by using the condition number of the matrix.

IV. Displacement-sensing link shells

The link shells are designed to detect the movements in all 6 degrees of freedom. To this end, a passive 6-dof parallel mechanism based on the Gough-Stewart architecture [12] is used. The passive mechanism has a stable neutral configuration, which it returns to when unloaded. This is accomplished using springs mounted on the legs of the mechanism. The stiffness of the springs and the preload is adjusted to ensure that the mechanism does not move under the effect of the weight of the shell and that the interaction forces perceived by the user are appropriate. Since the serial robot on which the shells are mounted is always trying to follow the motion measured by the shell sensors —i.e., trying to keep the sensing mechanism in its neutral configuration—, the range of motion of the passive mechanism need not be very large with respect to the size of the mechanism. The architecture of the Gough-Stewart platform is modified in order to have the effector around the base instead of over it such that the shell surrounds the link. The architecture is shown in Fig. 4 together with a photograph of the prototype. Infrared distance sensors in the cylinders are used to measure the length of the cylinders and these lengths can be used to compute the direct kinematics of the Gough-Stewart platform constituting the sensor and find the displacement of the shell. The solution of the direct kinematics of a parallel mechanism has been studied in many references (e.g. [13][14][15]). Numerical solutions are available, for example using the Newton-Gauss algorithm [16]. Moreover, in this application, the mechanism is always relatively close to the reference configuration and does not reach singular configurations, which ensures that the numerical procedure always converges and is very efficient.

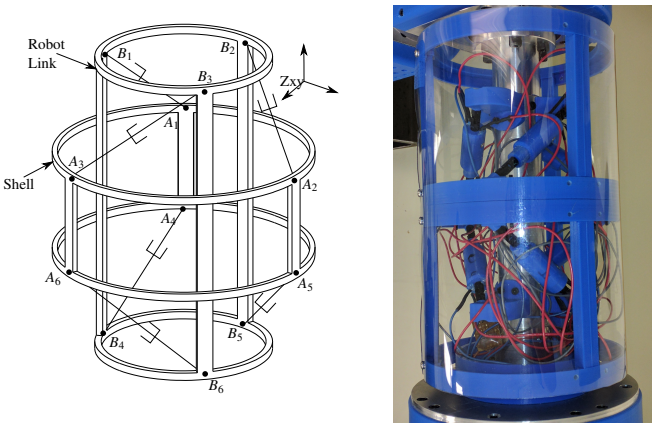

Fig. 4. Architecture of the displacement sensor, where B_i is the ith attachment point on the robot link and A_i is the ith attachment point on the mobile shell. The line connecting A_i and B_i represents the spring-loaded linear position sensors. A photograph of the prototype is shown on the right hand side.

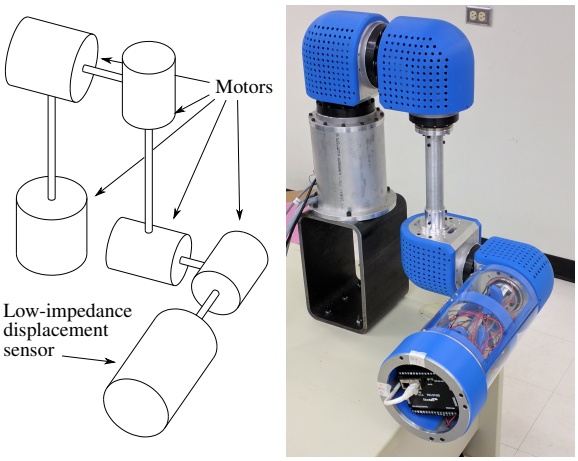

Fig. 5. Architecture of the experimental 5-dof robot with the low-impedance displacement sensor.

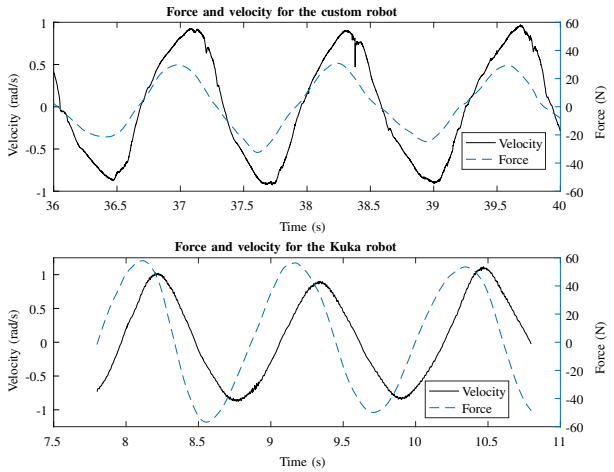

Fig. 6. Force and velocity comparison between the sensing device and the Kuka LWR for a similar movement using only the first 5 joints of the Kuka LWR robot.

V. Experimental validation

The 6-dof displacement-sensing link shell was tested on a custom-built 5-dof robot. Using a robot that has fewer dofs than the sensor itself demonstrates the effectiveness of the mapping algorithm presented in section III. The general architecture of the serial robot is presented in Fig. 5. The architecture is based on two clusters of motors: one with three motors and the other with two motors.

As shown in Fig. 5, the prototype of the sensor was mounted on the last link of the 5-dof robot and tests were conducted to assess the performance of the proposed concept. One of the main features of the approach used in this paper is, as stated previously, the very low impedance of the sensing device. This allows the user to move the robot using a very small force. The force required to move the robot is compared to the force required to move a Kuka LWR robot. A force sensor is mounted on each robot and used to input a force on the robot which in turn generates a movement.

The results of the experiments conducted with the two robots are shown in Fig. 6, where the interaction force and the velocity of the robot are plotted as a function of time for an oscillating motion. It can readily be observed from the figure that approximately twice as much force is necessary in order to produce similar speeds at a similar frequency with the Kuka LWR robot. Since the displacement sensor has a very low impedance, the force required to produce a given acceleration is lower and this force can be tuned by changing the pre-load or the springs used in the passive mechanism. Another important observation is the phase difference between the velocity and the force applied. For the Kuka LWR, the velocity lags behind the force applied due to its higher impedance, whereas the sensing device's velocity almost stays in phase with the force. The phase difference for the Kuka LWR in Fig. 6 is between 0.11-0.18s while for the LISD it is between 0.07-0.1s. Having a small phase difference between the applied force and the movement is directly related to the comfort of the user. When the phase difference is large, the user may feel as if he is fighting the robot when trying to apply an acceleration. A smaller phase difference means a much more responsive feeling and a better sense of control on the movement. When working for a longer period of time with the robot, the large phase difference can become tiring for the user because he will feel like he is trying to move a large inertia. This result illustrates the benefit of a low-impedance interface, which is confirmed by the comfort perceived during the experimental tests.

VI. Conclusion

Lightweight multi-degree-of-freedom displacement-sensing link shells for the intuitive physical human-robot interaction are proposed in this article. This concept yields a low impedance interface since the user is no longer in contact with the structural components of the robot. The controller used to implement the concept was briefly presented and the low-impedance position sensor, which is based on a Gough-Stewart platform architecture was introduced. Experiments conducted with a 5-dof robot on which the 6-dof sensor was mounted were reported. The effectiveness of the concept was demonstrated by comparing the interaction forces with those measured while interacting with a Kuka LWR robot and noting the improved tracking characteristics. Future work includes the extension of the robot to a 7-dof architecture and the integration of low-impedance sensors on all of its links.

References

[1] G. Raiola, C. A. Cardenas, T. S. Tadele, T. de Vries, and S. Stramigioli, "Development of a safety-and energy-aware impedance controller for collaborative robots," *IEEE Robotics and Automation Letters*, vol. 3, no. 2, pp. 1237–1244, 2018.

[2] A. Lecours, B. M. St-Onge, and C. Gosselin, "Variable admittance control of a four-degree-of-freedom intelligent assist device." in *Proc. IEEE Int. Conf. Robot. Autom.*, 2012, pp. 3903–3908.

[3] G. Grunwald, G. Schreiber, A. Albu-Schaffer, and G. Hirzinger, "Touch: The direct type of human interaction with a redundant service robot," in *Robot and Human Interactive Communication, 2001. Proceedings. 10th IEEE International Workshop on*. IEEE, 2001, pp. 347–352.

[4] R. Q. van der Linde and P. Lammertse, "Hapticmaster–a generic force controlled robot for human interaction," *Industrial Robot: An International Journal*, vol. 30, no. 6, pp. 515–524, 2003.

[5] A. Sharon, N. Hogan, and D. E. Hardt, "High bandwidth force regulation and inertia reduction using a macro/micro manipulator system," in *Robotics and Automation, 1988. Proceedings., 1988 IEEE International Conference on*. IEEE, 1988, pp. 126–132.

[6] O. Khatib, "Augmented object and reduced effective inertia in robot systems," in *American Control Conference, 1988*. IEEE, 1988, pp. 2140–2147.

[7] P. D. Labrecque, J.-M. Haché, M. Abdallah, and C. Gosselin, "Low-impedance physical human-robot interaction using an active–passive dynamics decoupling," *IEEE Robotics and Automation Letters*, vol. 1, no. 2, pp. 938–945, 2016.

[8] P. D. Labrecque, T. Laliberté, S. Foucault, M. E. Abdallah, and C. Gosselin, "uMan: A low-impedance manipulator for human–robot cooperation based on underactuated redundancy," *IEEE/ASME Transactions on Mechatronics*, vol. 22, no. 3, pp. 1401–1411, 2017.

[9] N. Badeau, C. Gosselin, S. Foucault, T. Laliberté, and M. E. Abdallah, "Intuitive physical human-robo interaction: using a passive parallel mechanism," *IEEE Robotics & Automation Magazine*, vol. 1070, no. 9932/18, 2018.

[10] N. Lauzier, M. Grenier, and C. Gosselin, "Two-dof cartesian force limiting device for safe physical human-robot interaction," in *Robotics and Automation, 2009. ICRA'09. IEEE International Conference on*. IEEE, 2009, pp. 253–258.

[11] A. S. Deo and I. D. Walker, "Overview of damped least-squares methods for inverse kinematics of robot manipulators," *Journal of Intelligent and Robotic Systems*, vol. 14, no. 1, pp. 43–68, 1995.

[12] D. Stewart, "A platform with six degrees of freedom," *Proceedings of the Institution of Mechanical Engineers*, vol. 180, no. 1, pp. 371–386, 1965.

[13] P. Nanua, K. J. Waldron, and V. Murthy, "Direct kinematic solution of a stewart platform," *IEEE transactions on Robotics and Automation*, vol. 6, no. 4, pp. 438–444, 1990.

[14] S.-M. Song *et al.*, "Forward kinematics of a class of parallel Stewart platforms with closed-form solutions," in *Robotics and Automation, 1991. Proceedings., 1991 IEEE International Conference on*. IEEE, 1991, pp. 2676–2681.

[15] R. Nair and J. H. Maddocks, "On the forward kinematics of parallel manipulators," *The International Journal of Robotics Research*, vol. 13, no. 2, pp. 171–188, 1994.

[16] J. Angeles and J. Angeles, *Fundamentals of robotic mechanical systems*. Springer, 2002, vol. 2.